SAND2016-8850C

Developing Imaging Capabilities of Multi-Channel Detectors Comparable to Traditional X-Ray Detector Technology for Industrial and Security Applications

Edward S. Jimenez[a], Noelle M. Collins[a], Erica A. Holswade[a], Madison L. Devonshire[b] and Kyle R. Thompson[b]

[a]Sandia National Laboratories, PO BOX 5800, Mail stop 0932, Albuquerque NM, USA;
[b]Sandia National Laboratories, PO BOX 5800, Mail stop 0555, Albuquerque NM, USA;

ABSTRACT

This work will investigate the imaging capabilities of the Multix multi-channel linear array detector and its potential suitability for big-data industrial and security applications versus that which is currently deployed. Multi-channel imaging data holds huge promise in not only finer resolution in materials classification, but also in materials identification and elevated data quality for various radiography and computed tomography applications. The potential pitfall is the signal quality contained within individual channels as well as the required exposure and acquisition time necessary to obtain images comparable to those of traditional configurations. This work will present results of these detector technologies as they pertain to a subset of materials of interest to the industrial and security communities; namely, water, copper, lead, polyethylene, and tin.

1. INTRODUCTION

The objective of this work is to create a color X-ray Radiography and Computed Tomography (CT) capability at Sandia National Laboratories for R&D in industrial, security, and general non-destructive testing applications at almost arbitrary scale and configuration. Also known as Energy-Discriminated or Energy-Resolved Imaging, the potential applications that are relevant to Sandia National Laboratories' Multi-Mission environment include verification & validation, high-magnification/high-energy CT, quality assurance, anomaly/target detection, checkpoint security, material identification, and real-time multi-energy CT.

It is well known that traditional CT approaches that utilize Bremmstrahlung radiation sources undoubtedly will contain some level of artifacts, noise, or both due to beam-hardening, which is caused by the non-linear preferential absorption fo lower energy X-rays compared to the high energy X-rays which leads to an increase in the average energy incident on the Xray detector versus the average energy incident on the object. Many of these artifacts could potentially be mitigated by pre-hardening or post-hardening the radiation before the radiation impinges the detector; however, this does not completely eliminate the noise or adequately address the challenge. Furthermore, hardening of the radiation may cause additional issues such as, reducing contrast of the lower attenuating materials, introduce additional scatter due to the hardening filter, as well as potentially increase scan time due to the reduction in photon flux at the detector.

Other applications that could benefit from energy-discriminated/Resolved imaging includes materials classification/identification such as that done by Jimenez et. Al.,[1] Collins et. Al.,[2] and Wurtz et. Al.[3] in which dual-energy or multi-energy approaches could potentially be improved by leveraging the energy-resolved data. Energy-resolved imaging has already been demonstrated to show great promise in the medical community such as in Dual-energy Radiography,[4] and in the detection of neoplastics in breast tissue by Johns and Yaffe.[5]

Further author information: (Send correspondence to E.S.J)
E.S.J.: E-mail: esjimen@sandia.gov, Telephone: 1-505-284-9690
K.R.T.: E-mail: krthomp@sandia.gov

2. BACKGROUND

This work will demonstrate the performance of an energy-resolved linear array that was recently acquired and utilize two potential applciations as an indicator of potential performance. The two applications will be that of attenuation profile with respect to energy estimation investigated by Collins et. Al.[2] and Jimenez et. Al.[1,6,7] and the work done at Lawrence Livermore National Laboratory (LLNL) by Wurtz et. Al.[3] with the LLNL-Metric for materials classification.

Although other applications were mentioned above as other examples that could potentially be improved by energy-resolved imaging, they were not considered in this work as they require additional hardware such as staging systems and other hardware that has not been integrated into the imaging system that is currently under assembly at the time of this work. One the required hardware has been integrated, a follow-up effort will be reported.

2.1 Materials Identification

Work done by Collins et. Al.[2] to verify apporaches porposed by Jimenez et. Al.,[1,6,7] presented an experimental apporach to acquire X-ray transmission data from a single pixel Cadmium-Telluride (CdTe) detector creating over one thousand channels of binned X-ray energy data for energies up to 450keV. Although this priliminary work showed that further work much be conducted; much promise was shown by demonstrating that the characteristic K-edges in the attenuation profile can be extracted for some of the materials of interest.

Collins et. Al. attempt two methods of extracting the attenuation profile with respect to energy, the first is a direct calculation based on Beer's Law, the detector reading without material present between the source and detector, and a detector reading with the material of interest present. Although it was expected to encounter challenges due to noise for the low-end channels and pulse pile-up for the high-end channels, Collins et. Al. were able to resolve the K-edges for some materials as was demonstrated by the numerical simulations performed by Jimenez et. Al.

2.2 LLNL-Metric

Wurtz et. Al. at Lawrence Livermore National Laboratory proposed a dual-energy metric that does not depend on the imaging system geometry or material/sample thickness to classify materials of interest for cargo screening applications.[3] This evolution on dual-energy Radiography methods measures:

$$\left(\frac{\frac{I}{I_0}|_l}{\frac{I}{I_0}|_h},\ ln\left(\frac{I}{I_0}|_l\right)\right),$$

where $\left(\frac{I}{I_0}\right)|_l$ is an image ratio of a light image and object present image at a low-energy setting and similarly, $\left(\frac{I}{I_0}\right)|_h$ is the same ratio acquired at some higher energy setting. This example is being used as a performance metric as energy-resolved imaging can directly integrate the LLNL-Metric by using single channels or sums of subsets of channels to create high and low-energy reading for I and I_0; thus allowing a potentially faster, simpler, or more efficient acquistion to take place as well as with potentially lower dose as only a single energy resolved measurement is required.

3. APPROACH

This work proposes using energy-resolved imaging to improve various data quality issues in tradional X-ray Radiography and CT methods. Given energy-resolved images, one can leverage the individual binned channel data to effectively acheive almost mono-energetic image data that is beyond the capabilities of any filtering configuration on a Bremmstralung source, reject noisy bins/regions, and potentially reduce dose and scan-time. Although these methods have already benefited various medical applications as mentioned above; they have not been necessarily proven for industrial and security applications.

4. EXPERIMENTAL DESIGN

This work will demonstrate performance of the recently acquired Multix Detection ME100 detector using a 450kVP Comet X-ray Source as well as 5 sheets of materials of interest: Tin with a thickness of 0.813mm, Copper with a thickness of 0.2mm, Lead with a thickness of 0.76mm, Polyethylene with a thickness of 13.5mm, and Water in a plastic container with a thickness of 59.2mm. These materials were chosen as the work by Jimenez et. al.[1] focused on these materials while Collins et. al.[2] focused on the first three. The Multix Detector consists of 5 modules, each with 128 pixels for a total of 640 pixels. The modules are arranged side-by-side to form a linear array approximately 0.5 meters wide with module pixels having a 0.8mm pixel pitch, adjacent pixels on different modules have a wider pitch that is currently unknown to the authors of this work. According to the documentation, each pixel in the ME100 module is capable of binning data into 128 channels which span a 300keV energy window with each channel uniformly spaced across the energy window. Each pixel can handle up to $1M$ counts per second. Many settings typical to energy resolved detectors are fixed by the manufacturer such as gain; other information, such as deadtime/livetime are not reported by the hardware. It is unknown to the authors whether the ME100 modules perform any type of scatter rejection, correction, or calibration and wish to gain insights to these questions with our measurements. As the imaging system is still under construction, only line readings (as opposed to full 2D images) will be acquired; the geometry of the system was made to replicate the geometry that Collins et. Al. utilized and will compare results from this work to those of Collins et. Al. when possible.

The data acquisition will vary the x-ray source energy settings from 50 to 300keV in 50keV increments and will test multiple currents for each measurement and will have a constant exposure time of 1 second. This work will measure detector count rate scalability across current and energy, performance on the Collins et. Al. direct calculation for each of the materials listed above, performance of the LLNL-Metric for each of the materials of interest, measurement of the mean spectrum output across pixels for each of the materials of interest as well as through air, measurement of normalized spectra at each energy for various currents, and measurment of signal-to-noise with respect to both energy channel and pixel position.

5. RESULTS

5.1 Count Rate

Count rates of the Energy Resolved Detector (ERD) at various energies and currents are shown in figs. 1 to 6. Each of these plots have a zero-intercept line and general line fit to the data to show the scalability with respect to current. Each data point is a sum of all pixel counts across the 640 pixel araray; all energies show good scalability as current is varied as well as no sign of saturation.

5.2 Direct Calculation

Direct estimates the the attenuation profile with respect to energy from Multix detector data are shown in figs. 7 and 8 for Lead, Polyethylene, and Water respectively. Direct estimates of the attenuation profile from Multix Detector data are shown next to the Amptek detector estimates performed by Collins et. Al.[2] for Copper and Tin in figs. 9 and 10 respectively. It is clear from fig. 7 that it is indeed possible to estimate the characteristic K-edges of materials as was shown in Jimenez et. Al.[1] and Collins et. Al.;[2] however, from figs. 9 and 10, there is clearly some corrections that need to be made to the Multix raw data as the estimates seem to be very inaccurate when compared to the estimates of Collins et. Al.

5.3 Lawrence Livermore National Laboratory Metric

The LLNL-Metric is shown in figs. 11 and 12. The plot shown in fig. 11, is the traditional visualization of the metric with fig. 12 being another visualization to show how the metric various as the higher energy is varied; in this case, the lower energy was selected to be the channel that corresponds to the 150keV energy bin and every other bin with higher energy was used to calculate various metrics using various high energies. For the given

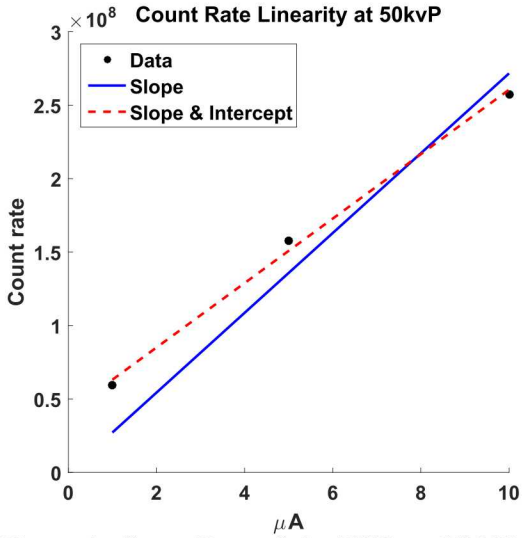

Figure 1: Count Rate of the ERD at 50kVP.

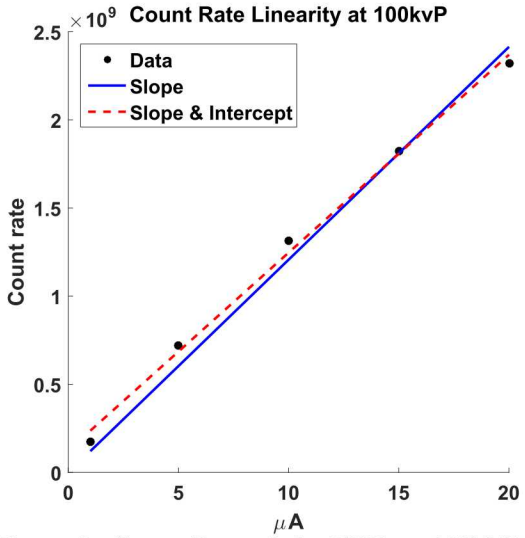

Figure 2: Count Rate of the ERD at 100kVP.

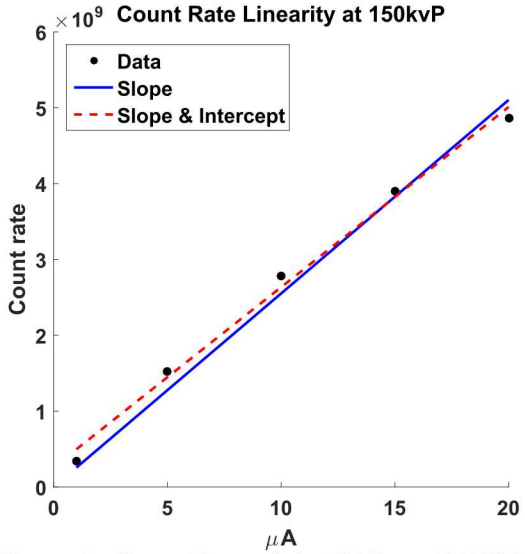

Figure 3: Count Rate of the ERD at 150kVP.

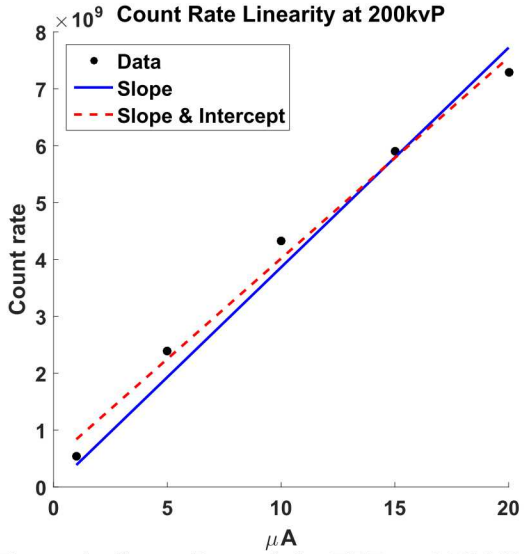

Figure 4: Count Rate of the ERD at 200kVP.

thicknesses, Multix data seems to show very good separation between materials when plotted in the traditional manner. Further work is needed to study variations with respect to thickness to completely determine its viability.

5.4 Mean Spectrum Output

The mean spectrum output for the materials of interest is shown in fig. 13. The characteristic peak for Tungsten is visible for the less attenuative materials and dissipates for the higher attenuative materials with signs of potential noise as Water and Lead seem to show comparable attenuating properties for 200-250keV.

5.5 Normalizaed Spectra

Normalized Spectra at 50keV increments are shown in figs. 14 to 19 for various current settings. For the figures corresponding to settings below 300kVP, it is clear that there is significant pulse pile-up in the data by the

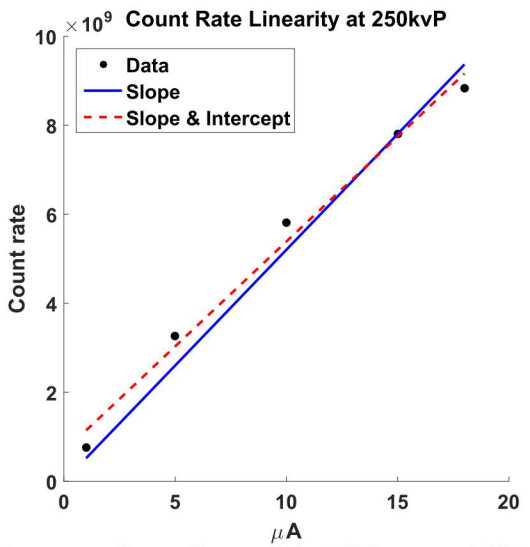

Figure 5: Count Rate of the ERD at 250kVP.

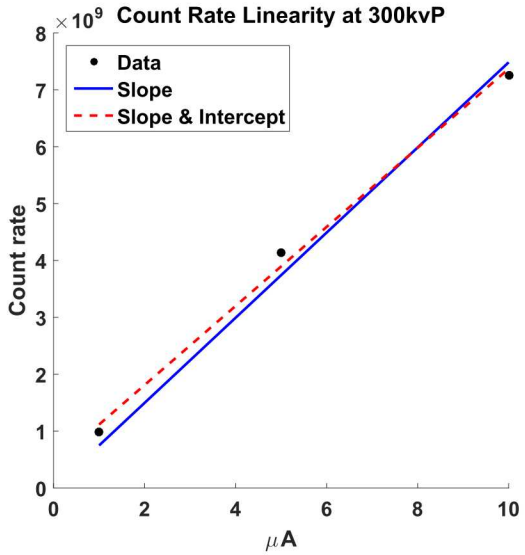

Figure 6: Count Rate of the ERD at 300kVP.

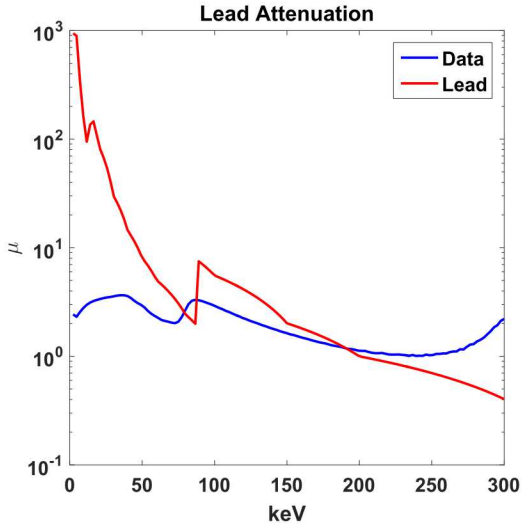

Figure 7: Direct estimate of the attenuation profile for Lead at 300kVP from the Energy Resolved Detector.

presence of counts above the settings for each acquisition as well as an underrepresentation of the low energy counts; ideally, for some reasonable current settings, when the spectra is normalized, each profile regardless of current setting should overlap with all profiles corresponding to the same kVP setting.

5.6 Signal-to-Noise

Signal-to-Noise with respect to pixel position is shown in fig. 20. The pixel SNR appears to be consistent across position; there appears to be a cyclical nature to the SNR, but more investigation is needed to find the cause. SNR with respect to energy is shown in fig. 21 and shows acceptable levels across a majority of the energy window with the best SNR being acheived for energies between 50-250keV and is possibly mostly due to noise in the system as well as pile-up.

6. CONCLUSIONS

This work has demonstrated early performance metrics with the Multix energy discriminating linear array and its potential viability as an R&D Non-Destructive Evaluation imaging system. While there is much work to be

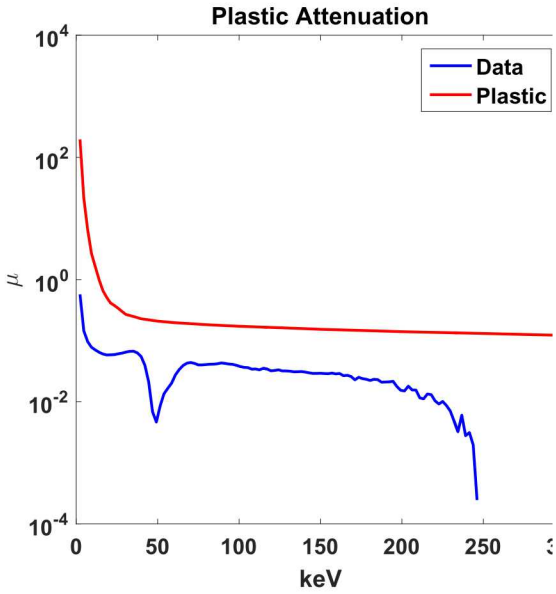

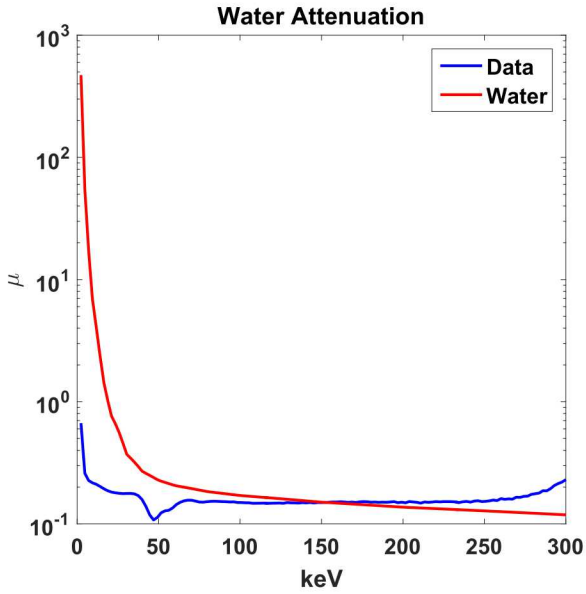

Figure 8: LEFT: Direct estimate of the attenuation profile for Polyethylene at 300kVP from the Energy Resolved Detector. RIGHT: Direct estimate of the attenuation profile for Water at 300kVP from the Energy Resolved Detector.

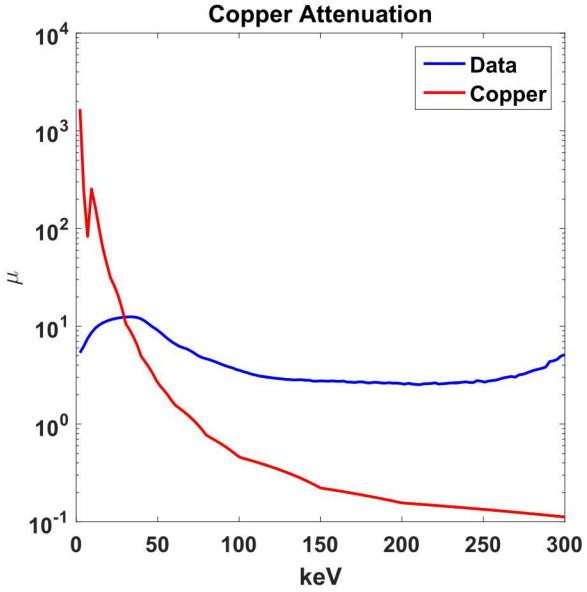

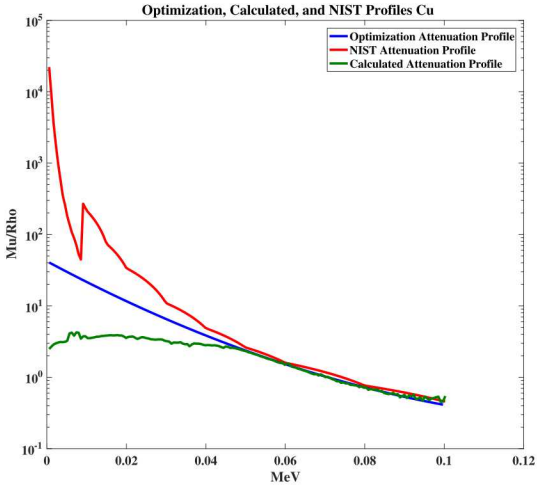

Figure 9: LEFT: Direct estimate of the attenuation profile for Coppper at 300kVP from the Energy Resolved Detector. RIGHT: Estimates from Collins et. Al. for Copper.[2]

done to investigate its full sensitivities as well as develop calibration and correction methods; the system holds promise in pushing the boundaries of technology and capabilities not just for Sandia National Laboratories, but for the entire Industrial and Security Non-Destructive Evaluation community. While many works have shown methods to spectrum correction,[8–10] it still needs to be investigated whether new approaches need to be developed for applications in the higher energy ranges. The utilization and integration of energy-resolved x-ray imaging will have and has already demonstrated widespread impact; work leveraging this technology includes Johns and Yaffe,[5] Tomita et. Al.,[11] Jimenez et. Al.[1] and Collins et. Al.[2] Additionally, this technology could impact other works that are based on Dual-energy approaches such as.[3,4,12]

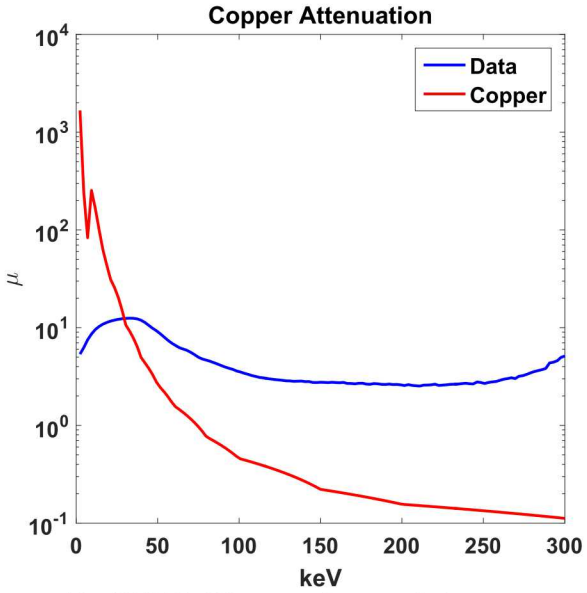

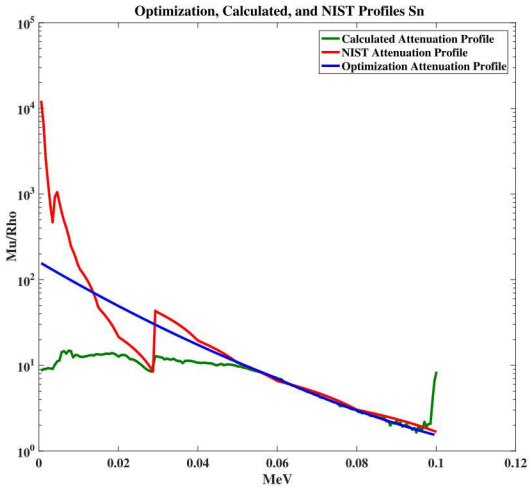

Figure 10: LEFT: Direct estimate of the attenuation profile for Tin at 300kVP from the Energy Resolved Detector. RIGHT: Estimates from Collins et. Al. for Tin.[2]

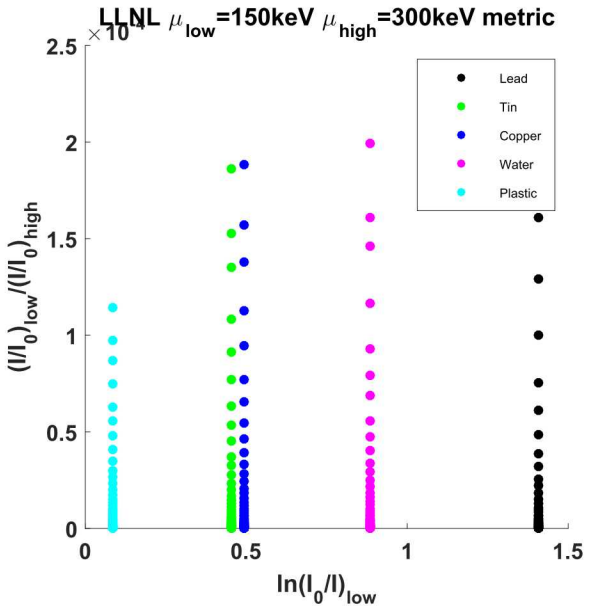

Figure 11: LLNL Metric for varying keV with 5 materials

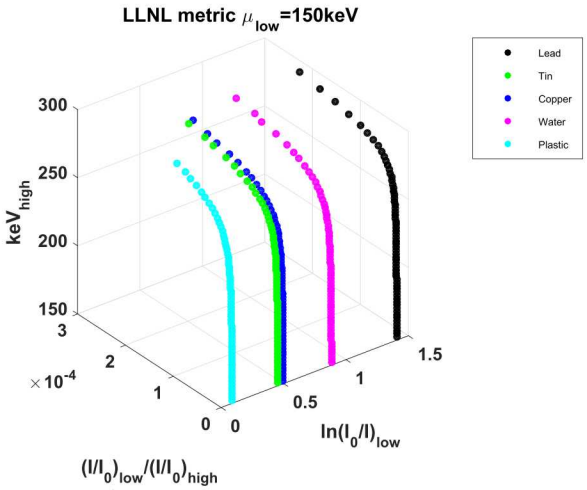

Figure 12: A 3D view of the LLNL Metric for varying keV.

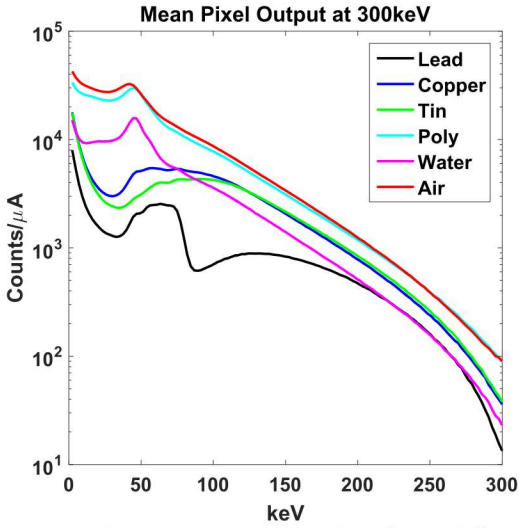

Figure 13: Mean pixel output with respect to energy bin for 5 different materials at 300 kVP.

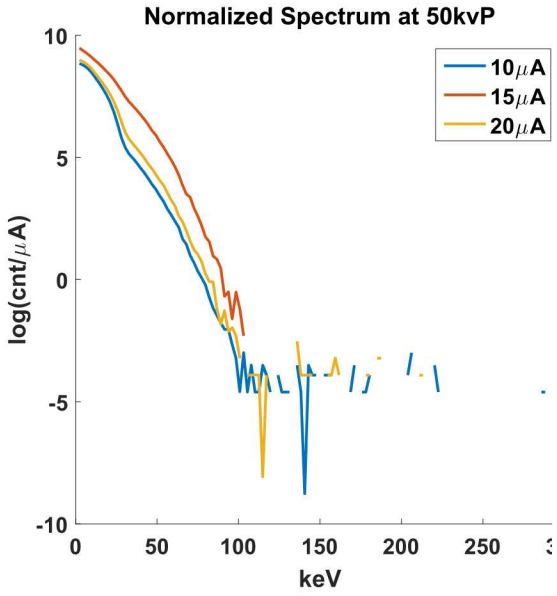

Figure 14: Normalized unfiltered spectra at 50kVP.

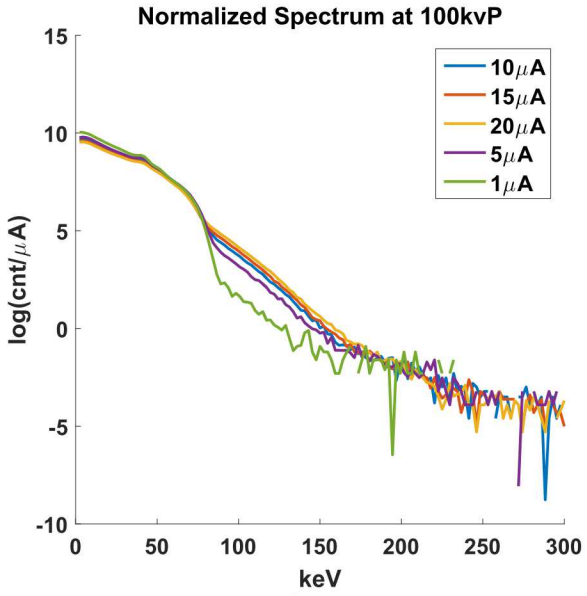

Figure 15: Normalized unfiltered spectra at 100kVP.

7. ACKNOWLEDGEMENTS

Sandia National Laboratories is a multi-mission laboratory managed and operated by Sandia Corporation, a wholly owned subsidiary of Lockheed Martin Corporation, for the U.S. Department of Energy's National Nuclear Security Administration under contract DEAC04-94AL85000.

REFERENCES

[1] Jimenez, E. S., Orr, L. J., and Thompson, K. R., "Object composition identification via mediated-reality supplemented radiographs," in [*IEEE Nuclear Science Symposium and Medical Imaging Conference*], (Nov. 2014).

[2] Collins, N. M., Thompson, K. R., and Jimenez, E. S., "An experiment for material classifications using multichannel radiographs," in [*Review of Progress in Quantitative Nondestructive Evaluation*], (Jul. 2016).

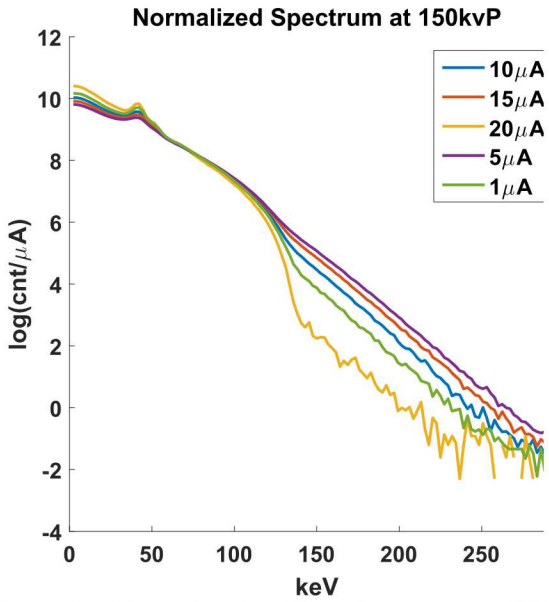

Figure 16: Normalized unfiltered spectra at 150kVP.

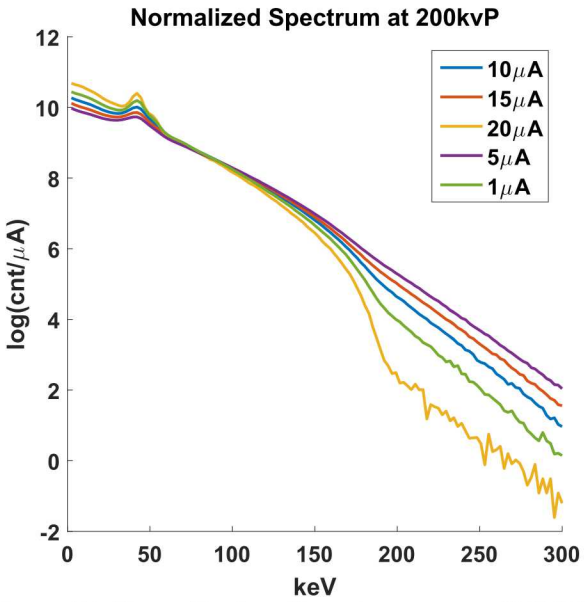

Figure 17: Normalized unfiltered spectra at 200kVP.

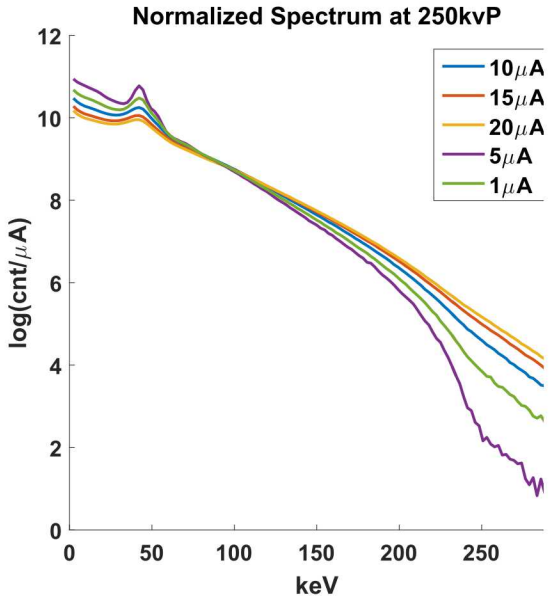

Figure 18: Normalized unfiltered spectra at 250kVP.

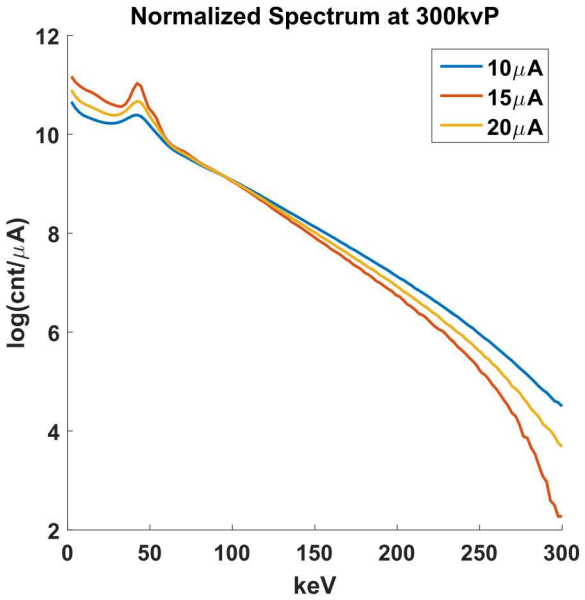

Figure 19: Normalized unfiltered spectra at 300kVP.

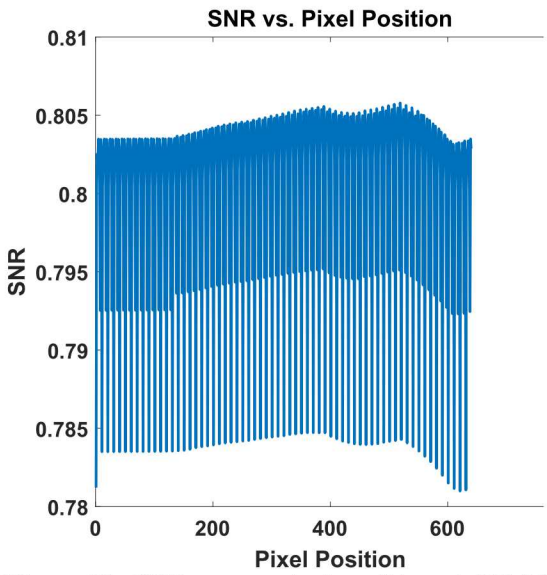

Figure 20: SNR versus pixel position at 300 kVP.

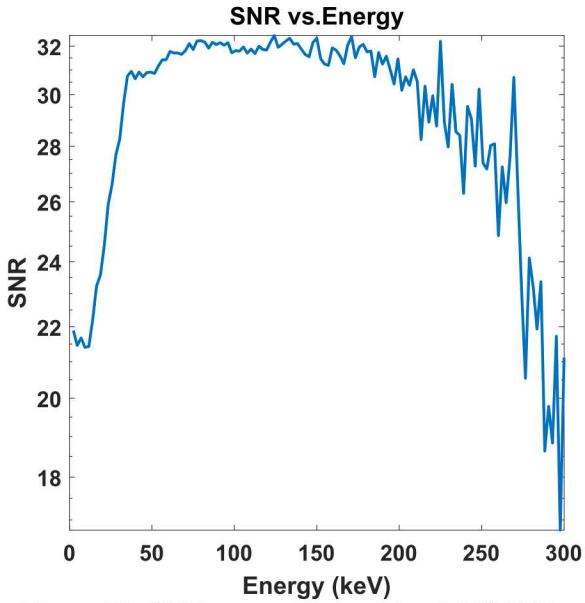

Figure 21: SNR versus energy bin at 300 kVP.

[3] Wurtz, R., Walston, S., Dietrich, D., and Martz, H., "Metrics for developing an endorsed set of radiographic threat surrogates for jinii/caars," tech. rep., Lawrence Livermore National Laboratory (LLNL), Livermore, CA (2009).

[4] Blake, G. M. and Fogelman, I., "Technical principles of dual energy x-ray absorptiometry," in [*Seminars in nuclear medicine*], **27**(3), 210–228, Elsevier (1997).

[5] Johns, P. C. and Yaffe, M. J., "X-ray characterisation of normal and neoplastic breast tissues," *Physics in medicine and biology* **32**(6), 675 (1987).

[6] Jimenez, E. S., Orr, L. J., Morgan, M. L., and Thompson, K. R., "Exploring mediated reality to approximate x-ray attenuation coefficients from radiographs," in [*Penetrating Radiation Systems and Applications XIV at SPIE Optics+Photonics 2014*], (Aug. 2014).

[7] Jimenez, E. S., Thompson, K. R., and Orr, L. J., "Utilization of virtualized environments for efficient x-ray attenuation approximation," in [*ASNT Research Symposium*], (Mar. 2014).

[8] Brambilla, A., Ouvrier-Buffet, P., Rinkel, J., Gonon, G., Boudou, C., and Verger, L., "Cdte linear pixel x-ray detector with enhanced spectrometric performance for high flux x-ray imaging," *IEEE Transactions on Nuclear Science* **59**(4), 1552–1558 (2012).

[9] Sabbatucci, L., Scot, V., and Fernandez, J. E., "Multi-shape pulse pile-up correction: the mcppu code," *Radiation Physics and Chemistry* **104**, 372–375 (2014).

[10] Taguchi, K., Frey, E. C., Wang, X., Iwanczyk, J. S., and Barber, W. C., "An analytical model of the effects of pulse pileup on the energy spectrum recorded by energy resolved photon counting x-ray detectors," *Medical physics* **37**(8), 3957–3969 (2010).

[11] Tomita, Y., Shirayanagi, Y., Matsui, S., Aoki, T., and Hatanaka, Y., "X-ray color scanner with multiple energy discrimination capability," in [*Optics & Photonics 2005*], 59220A–59220A, International Society for Optics and Photonics (2005).

[12] Primak, A., Giraldo, J. R., Liu, X., Yu, L., and McCollough, C. H., "Improved dual-energy material discrimination for dual-source ct by means of additional spectral filtration," *Medical physics* **36**(4), 1359–1369 (2009).